Articles in PresS. J Neurophysiol (August 6, 2008). doi:10.1152/jn.90531.2008

COMPLEX ORGANIZATION OF HUMAN PRIMARY MOTOR CORTEX: A HIGH RESOLUTION fMRI STUDY

Abbreviated title: Human motor cortex

Jeffrey D. Meier, Tyson N. Aflalo, Sabine Kastner, Michael S. A. Graziano

Address for all authors: Department of Psychology, Princeton University, Princeton NJ 08544

Corresponding author:

Michael Graziano, Department of Psychology, Green Hall, Princeton University, Princeton, NJ 08544.

Phone: 609 258 7555. Fax: 609 258 1113. Email: Graziano@princeton.edu.

Abstract

A traditional view of the human motor cortex is that it contains an overlapping sequence of body part representations from the tongue in a ventral location to the foot in a dorsal location. In the present study, high resolution functional magnetic resonance imaging (1.5 X 1.5 X 2 mm) was used to examine the somatotopic map in the lateral motor cortex of humans, to determine whether it followed the traditional somatotopic order or whether it contained any violations of that somatotopic order. The arm and hand representation had a complex organization in which the arm was relatively emphasized in two areas, one dorsal and the other ventral to a region that emphasized the fingers. This violation of a traditional somatotopic order suggests that the motor cortex is not merely a map of the body but is topographically shaped by other influences, perhaps including correlations in the use of body parts in the motor repertoire.

Key words: primary motor cortex; M1; somatotopic map; motor control; hand; arm.

Introduction

The monkey motor cortex contains a progression of body part representations along the precentral gyrus. This map of the body differs from a simple linear arrangement of body parts in at least two ways. First, the map has a blurred, overlapping somatotopy in which the representations of different body parts are intermingled (e.g. Donoghue et al. 1992; Gould et al. 1986; Park et al. 2001; Sessle and Wiesendanger 1982; Woolsey et al. 1952). For example, the fingers do not have separate cortical zones but are represented in an overlapping manner (Schieber and Hibbard 1993). This representational overlap may aid in the functional integration among body parts during normal, learned behavior (e.g. Nudo et al. 1996). Consistent with this view, when a site in the monkey motor cortex is electrically stimulated on a behaviorally relevant time scale, the resulting movement combines joints and muscles in a manner resembling a coordinated action (Graziano et al. 2002).

A second deviation from a simple somatotopic map is that, even given a blurred, overlapping progression of body parts from the face to the leg, the progression does not follow a simple order. A reversal in the body representation was reported in the monkey by Kwan et al. (1978) and confirmed by Park et al. (2001). The fingers are emphasized in a core region and the arm is emphasized in a half ring surrounding the core, violating a simple body map. At first glance the core and surround organization appears to conflict with the blurred, overlapping property of the motor cortex map summarized above. If the arm and hand are represented in an overlapping manner, how can they be separated into a

core hand area and a surrounding arm area? This core and surround organization, however, is probably one of relative emphasis, not absolute representation. Both the arm and hand appear to be represented in both cortical sectors, but the fingers are relatively more emphasized in the core area and the arm in the surround area. As a result, with electrical stimulation of cortex, it is possible to lower to stimulation current until only the strongest representation remains above the detection threshold. This "tip of the iceberg" phenomenon, in which only the tip of the movement ensemble is detected, might explain the discrete maps of a core and surround organization obtained by Kwan et al. (1978) and confirmed by Park et al. (2001).

One interpretation of the core-and-surround organization is that joints that interact in the motor repertoire are represented as near as possible to each other on the cortical surface, allowing for more efficient lateral interactions. In support of this hypothesis, the core-and-surround organization can be reproduced by a model of the motor cortex that minimizes distance between functionally related representations (Aflalo and Graziano 2006; Graziano and Aflalo 2007). In effect, the map is mixed and swirled in a way that most effectively serves the statistics of the animal's normal movement repertoire. In this interpretation, therefore, both complex properties of motor cortex, the overlapping nature of the map and the core and surround organization, stem from the same cause. They both facilitate the interaction among body parts. These functional interpretations, however, are speculations. The data show only that, whatever the functional significance, the monkey motor cortex contains both of these complexities in its somatotopic organization.

The human brain contains at least the first of these two complexities. The map is highly overlapping (Penfield and Boldrey 1937). For example, in human functional

imaging studies, the fingers are represented in an overlapping manner (Indovina and Sanes 2001; Sanes et al. 1995). Each finger, however, may have a local cortical hot spot in which it is emphasized, the hot spots arranged in strict somatotopic order (Beisteiner et al. 2001; Dechent and Frahm 2003; Hlustik et al. 2001; Kleinschmidt et al. 1997).

It is not known if the second complexity of the motor map described in monkeys, the core and surround organization, is also present in humans. Are the arm and hand representations so intermingled that no areas emphasizing one or the other body part can be distinguished; is the arm emphasized dorsally to the finger representation as in a standard somatotopic order; or is the arm emphasized both dorsally and ventrally to the finger representation as in the monkey brain? The purpose of the present experiment was to use high resolution fMRI to map the human motor cortex and ask whether it has a core-and-surround organization, such as in the monkey motor cortex, or any other violation of the standard somatotopic order.

Materials and Methods

Subjects and task

Five healthy right-handed subjects (3 males; 22-39 years of age) participated in the study, which was approved by the Institutional Review Panel of Princeton University. All subjects were in good health with no history of psychiatric or neurological disorders and gave their informed written consent. Subjects lay supine on the horizontal scanner bed with their heads surrounded by foam to reduce head movements and performed an instructed movement task. Analyses were carried out in individual subjects, thereby

justifying the small number of subjects typically used in cortical mapping literature (e.g. Sereno et al. 1995; Schneider et al. 2004). Single subject approaches are advantageous over methods that average among many subjects, because averaging blurs or removes fine features of the map that are not fully aligned among subjects given inter-subject variability.

The task cues were words projected from a PowerLite 7250 liquid crystal display projector (Epson, Long Beach, CA) outside the scanner room onto a translucent screen located at the end of the scanner bore. Subjects viewed the screen at a total path length of 60 cm through a mirror attached to the head coil. At the start of each movement condition, a word was presented at the center of the screen indicating the movement to be performed. For example, "tongue" was presented to instruct tongue movements. After 2 s the word disappeared and a central black fixation dot appeared. The dot blinked at a rate of 2 Hz (0.25 s on and 0.25 s off). The subject was required to fixate the dot and perform the instructed movement in synchrony with the blinking of the dot. For example, the tongue movement required moving the tongue forward in the mouth on one appearance of the dot, leaving the tongue in the forward position while the dot disappeared, retracting the tongue backward in the mouth on the next appearance of the dot, leaving the tongue in the back position while the dot disappeared, then moving the tongue forward again on the next appearance on the dot. Each cycle of the movement (tongue forward and tongue backward) was therefore cued by two dot flashes and lasted 1 s, a speed of movement that was found to be comfortable and easy to perform in pilot tests. After 6 s (12 dot flashes) the movement phase ended and the instruction for the next movement condition appeared.

During performance of the task the subject lay in a standard posture moving nothing but the instructed body joint. In this standard posture, the right arm was held such that the elbow was resting on the scanner bed, the elbow was bent at about a 135 degree angle such that the hand was lifted above the bed, the wrist was straight, the palm faced the midline of the body, and the fingers were stationary in a clawed posture without touching each other. Ten different movements were performed, all in synchrony with the flashing fixation dot.

Tongue: As described above, the tongue was moved alternately forward and backward in the mouth, while the lips and jaw remained still.

Lips: The lips were alternately pursed forward and then drawn back to the teeth.

Squint: The subject squinted the right side of the face, tensing the muscles around the eye without closing the eye, and then relaxed the face.

Hand: The fingers of the right hand were flexed toward each other, without touching, and then extended away from each other.

Wrist A: The wrist was flexed and then extended.

Wrist B: The wrist was adducted (rotated toward the thumb side) and then abducted (rotated toward the pinky side).

Forearm: The forearm was pronated (rotated such that the palm faced down) and then supinated (rotated such that the palm faced up).

Elbow: The elbow was extended to about 145 degrees and flexed to about 120 degrees.

Foot: The toes on the right foot were curled and uncurled.

Saccade: The fixation dot was presented initially in the center of the screen as for all other conditions. It flashed at 2 Hz as for all other conditions. However, at each onset after the first onset, the dot appeared randomly at any of 25 possible locations on the screen forming a 5x5 grid with 5 degrees of visual angle between adjacent grid locations. The dot therefore gave the impression of jumping about the screen randomly, one jump every 0.5 s. The subject was required to saccade to each new location of the dot as it appeared. A different random sampling of target locations was used for each saccade block in each scan.

Subjects performed a practice session first outside the scanner bore and then inside the scanner bore just prior to scanning, to ensure that they understood the instructions and that the movements were performed cleanly (for example that no accidental finger movement occurred during forearm rotation).

For each subject, eight scan runs were performed in one scanning session that was two hours long. Each run began with an 8 s rest period in which the word "rest" was displayed on the screen, followed by a series of 50 movement blocks. Each block was 8 s in duration including 2 s of instruction and 6 s of movement. Each run was thus 408 s. Within a run, all 10 movement types were presented, each type repeated 5 times in psudo-randomized order. The order was different for each of the 8 runs. In total, across runs, each movement type was repeated 40 times, the presentations balanced such that each movement type followed each other movement type approximately the same number of times.

Data acquisition

Images were acquired with a 3T Allegra head-dedicated MRI scanner (Siemens, Erlangen, Germany) using a standard birdcage head coil. Eight series of 204 volumes were acquired. All acquisitions used a gradient echo, echoplanar sequence with a 128 square matrix (20 axial slices, 2 mm thick, with a 1mm gap between slices, interleaved acquisition) leading to an in-plane resolution of 1.5 x 1.5 mm (FOV=192x192 mm, repetition time (TR), 2 s; echo time (TE), 41 ms; flip angle = 90°; 128X128 matrix). A partial Fourier factor of 7/8 was used to acquire an asymmetric fraction of *k*-space to reduce the acquisition time (see Schneider et al. 2004 for details). The acquisition volume was positioned to cover the motor cortex. Echoplanar images were compared with a coaligned, high-resolution anatomical scan of the whole brain taken at the end of each session (MPRAGE sequence; TR = 2.5 s; TE = 4.38 ms, flip angle = 8°; matrix, 256 X 256; 1 mm^3 resolution). To perform echo planar imaging undistortion (Cusak et al., 2003) an in-plane magnetic field map image was acquired (FOV=256x256 mm, 128 matrix, TR = 345 ms, TE = 5.06/8.06 ms, flip angle = 40 deg, bandwidth = 260 Hz/pixel). For cortical surface reconstructions, a high-resolution structural scan was acquired in a separate session (MPRAGE sequence, parameters as above, 6 acquisitions). All images were aligned to this high-resolution structural scan.

Data analysis

Individual subject analysis was performed using AFNI (Cox, 1996) (http://afni.nimh.nih.gov/afni), FreeSurfer (Dale et al. 1999; Fischl et al. 1999) (http://surfer.nmr.mgh.harvard.edu/), and SUMA (http://afni.nimh.nih.gov/). The first four images of each scan were eliminated from the analysis.

The functional images were motion corrected (Cox and Jesmanowicz 1999) to the image acquired closest in time to the anatomical scan and undistorted using the field map scan. Motion correction was especially important in this experiment because of the possibility that the instructed movements might induce small movements of the subject's head. The output of the motion correction algorithm indicated that head movement was negligible for all subjects. No systematic head movements were observed during any part of the task. For example, for subject 1, the mean translation vector within a run was 0.045 mm and the mean rotation vector within a run was 0.041 degrees. The mean change in head position was also calculated during each movement type and no significant differences were found among movement types. A similar lack of systematic head movement was found for all subjects.

Data were spatially smoothed with a Gaussian kernel of 4 mm (at full width, half maximum). Smoothing, though it may appear to contradict the benefit of high resolution scanning, does not simply throw away spatial information. Instead, it is routinely used to enhance signal-to-noise. The time course analyses (described below) were performed on unsmoothed data. The primary result of this experiment, the detection of a second small arm representation ventral to the hand representation, was the same regardless of whether smoothed data were used (as for the surface maps) or unsmoothed data was used (as for the time courses).

Regression analysis

First, for each subject, we obtained an average trace that showed the rise and fall of the hemodynamic response in motor cortex. The average trace was obtained in the

following way. The hemodynamic time series from 40 voxels were used. These voxels were selected throughout motor cortex, defined anatomically as the anterior bank of the central sulcus. Each individual time series was normalized to a peak value of 1. The normalization was performed to ensure that responses of different magnitudes, from different parts of motor cortex, would have equal weighting. These normalized time series were then averaged to obtain the mean hemodynamic response function. Figure 1 shows the mean hemodynamic trace for subject 1. We used this average as a model hemodynamic response in the regression analysis for subject 1. The curve obtained from the data was used as the model; it was not fitted to any parameterized function. For each subject, a unique, subject-based hemodynamic model was obtained.

A multiple regression analysis was performed on the hemodynamic responses after spatial smoothing. For each of the ten movement types, a square-wave function was generated representing the time intervals throughout the scan during which that movement was performed. This square-wave function was then convolved with the post-hoc model of the hemodynamic response based on individual subject data.

The convolved function was then used as a regressor in the multiple regression model. Ten of these regressors were included in the multiple regression model, corresponding to the ten movement types. Additional regressors were included in the model to factor out between-run changes in mean intensity and within-run linear drifts. For each voxel, the regression analysis returned ten β values, ten F values, and ten P values, one for each of the ten movement types (β values are displayed in Figure 2 for subject 1). Note that the multiple regression model does not compare each movement

type to a rest condition. Rather, it compares each movement type to all other movement types.

Winner-take-all map

For each subject, a surface map was generated to visualize the somatotopic progression in the motor cortex. First, a voxel was considered only if it had a positive hemodynamic response that passed a $P < 0.0001$ threshold (uncorrected for multiple comparisons) in the regression analysis described above. Second, for each of these voxels, a "winner-take-all" rule was used to assign a winning movement to that voxel. The winning movement was the movement that returned the largest F value (with a positive beta value) in the regression analysis. With this rule, even if several movements returned similar F values, one was always larger than the others, and therefore a winning movement could always be defined. Each voxel was assigned a display color based on the winning movement. Third, voxels that overlapped the cortical slab were displayed on an inflated brain map of the gray-white matter boundary (Figures 3 and 4). This winner-take-all method of displaying the data provides a convenient way to visualize the movement types that are most robustly represented at each cortical location. It provides an overview of the somatotopic progression. It does not, however, provide a complete description of the motor map. By assigning a single winning movement to each voxel, the method reveals only the tip of the movement "iceberg" at each cortical location. It does not show the manner in which one movement type overlaps with or grades into another. This overlapping of movement representations must be examined using different analyses, such as those described below.

Time series of fMRI signals

The winner-take-all maps allowed the motor cortex to be divided into regions that showed greatest hemodynamic signal covariance with one or another movement type. Based on these maps, points in cortex were selected near the center of each movement representation. Time series were then obtained to further assess the hemodynamic responses. Time series were calculated from the unsmoothed data in the following manner. Once a point on the cortical surface was selected, a normal line was drawn from that point through the cortical slab. Five adjacent voxels within the cortical slab were selected, the central one intersected by the normal line. The hemodynamic response throughout the scan time was averaged among those five voxels. Time series for individual movement types were then calculated. For example, the time series for the tongue movement response was calculated as follows. Tongue movement was performed 40 times throughout the scan. For each repetition, the time window beginning at the onset of the movement instruction and ending 22 seconds later was selected. The hemodynamic response during this window was then transformed into a percentage change from the value obtained at the start of that 22 sec time window. The 40 hemodynamic traces were then averaged together to produce a time series showing the mean hemodynamic response during and after tongue movement. A similar procedure was used to obtain time series for each of the ten movement types. (Example time series are shown in Figures 5 and 6).

Arm vs finger analysis

Typically the cortical representation of one movement graded into the next. To assess the gradual transition from the representation of finger movement to the representation of more proximal, wrist and forearm movement, the following method was used. First, voxels in the motor cortex were selected if the regression against finger movement, wrist A movement, wrist B movement, or forearm rotation was positive and if the P value passed the 0.0001 threshold. Second, for each of these voxels, a "finger-vs-arm" index was calculated based on the β values returned by the regression.

Finger-vs-Arm Index = [βfingers – ((βwrist A + βwrist B + βforearm)/3)] / [βfingers + ((βwrist A + βwrist B + βforearm)/3)]

This finger-vs-arm index varied between -1 and 1. A value of 1 indicated that the voxel was activated by the fingers and not the proximal movements of the arm. A value of -1 indicated that the voxel was activated by the proximal movements and not the fingers. A value of 0 indicated that the voxel was equally activated by the fingers and proximal movements. This index was then displayed as a color code on a flattened surface map. A separate map was obtained for each subject (Figure 7A-E).

Group analysis

The preceding analyses were all performed on individual subjects. This individual analysis prevented blurring across subjects that varied in the exact layout of their motor maps. However, despite the variance among subjects in the exact map layout, all subjects

showed a central finger representation bracketed by a dorsal and a ventral area that emphasized the arm. With proper alignment of the central finger representation, it should therefore be possible to average among subjects and arrive at a clearer picture of the surrounding arm representation. The average was performed in the following manner. For each subject, a flattened surface map of the motor cortex was generated. The β values for finger movement, obtained in the regression analysis, were plotted on this map. Only those β values that were positive and passed a $P < 0.0001$ threshold were plotted. The map of finger β values for subject 1 was used as a reference. The maps for subjects 2-5 were transformed to match the map of subject 1. The transformation was a standard affine transformation used in image analysis (Gonzalez and Woods, 2002) and included rotation, translations along the x and y axis, scaling along the x and y axis, and sheering. For example, for subject 2, the flattened map of the motor cortex was transformed to optimize the spatial correlation between the finger β values for subject 2 and for subject 1. In this fashion the map from subject 2 was warped until its finger area was optimally aligned with the finger area of subject 1. Once this alignment of finger areas was obtained for all subjects, the finger-vs-arm index was averaged across the five surface maps to produce a single group map of the finger-vs-arm index (Figure 7F).

Results

Overlapping somatotopy

A clear somatotopic organization was obtained in the motor cortex of each subject. Figure 2 shows the results of the regression analysis from subject 1 plotted onto

an inflated hemisphere. Each panel shows the results for one movement type. Only those voxels that showed a positive hemodynamic response and that passed a significance level of $P < 0.0001$ were plotted. Activity that correlated significantly with movement was found within the primary motor cortex in the anterior bank of the central sulcus. It was also found within the primary somatosensory cortex in the posterior bank of the central sulcus. Activity was also obtained on the pre- and post-central gyrus and within the inferior parietal cortex. The present report will focus on activations within the motor cortex.

Within the motor cortex in the anterior bank of the central sulcus, a rough, highly overlapping somatotopic progression was apparent, with the tongue represented ventrally (Figure 2A), the foot represented on the dorsal aspect and medial wall of the hemisphere (Figure 2I), and the other body parts arranged between. Each body part representation overlapped extensively with others, yet the general progression from tongue to foot was maintained. The saccadic eye movements (Figure 2J) evoked a large area of activation on the precentral gyrus anterior to the primary motor strip, consistent with the location of the frontal eye field (e.g. Kastner et al. 2007), and also activated a large area in the posterior parietal lobe.

One complexity to this map can be seen in the plots for wrist and forearm movement (Figure 2E, F, & G). In these maps, within the motor cortex in the anterior bank of the central sulcus, the activations were split, containing a larger dorsal zone and a smaller ventral zone. The cortical region activated by finger movements fit roughly between these dorsal and ventral arm zones. Thus the initial analysis suggests that the human motor cortex might have a type of core and surround organization.

Winner-take-all maps

Figure 3A provides a different view of the somatotopic progression for the same subject as in Figure 2. In this "winner-take-all" method of display, voxels were selected if the regression against any movement type was positive and significant at the $P < 0.0001$ threshold. For each of these selected voxels, a winner-take-all method was used to assign a winning movement, the movement that was associated with the highest F value. Voxels assigned to different movements were then given different colors for the display.

This winner-take-all display must be interpreted carefully. It does not reveal the map within the motor cortex. It shows only the peak movement representations. The true map is extensively overlapping, as shown in Figure 2. Nonetheless, the winner-take-all map is especially useful in revealing the topographic trends across the cortical surface. It shows the large-scale somatotopic progression in the anterior bank of the central sulcus and on the precentral gyrus. The order of progression from ventral to dorsal was approximately: tongue, lips, squint, wrist and forearm, fingers, a second representation of the wrist and forearm, elbow, and foot, with the foot activation largely hidden in this figure over the medial aspect of the hemisphere. A gap in the cortical map between the elbow activation and the foot activation presumably corresponded to the intervening body parts that were not tested in this experiment. A large zone activated by eye movement lay just anterior to the motor cortex somatotopic map, on the precentral gyrus. This map matches the traditional human motor map (e.g. Penfield and Boldrey 1937) in all respects except for the double representation of the wrist and forearm (indicated in blue and pink), one below and one above the finger representation (indicated in red).

Figure 3B shows the winner-take-all map from the same subject as in Figure 3A. The data in B were collected in a separate scan session two months later. The somatotopic pattern is strikingly similar in these two data sets, confirming that the results are reliable and consistent.

Figure 4 shows the winner-take-all maps from the remaining subjects. All subjects showed a similar pattern of activation in motor cortex, including a rough overall somatotopy and a core hand area that was bracketed both above and below by representations of the wrist and forearm.

Analysis of fMRI time series

The winner-take-all maps in Figures 3 and 4 assign a single, winning movement to each voxel and thus help to clarify the overall somatotopic trends. Those maps, however, do not provide information about representational overlap. For example, the finger area in Figure 3A (the red area) is shown as uniformly taken by the fingers, because the finger activation was statistically strongest there. Yet movement of the wrist, forearm and elbow also resulted in significant activity in this same region of cortex. This representational overlap is apparent in Figure 2, in which each movement activation is displayed separately. To better assess the manner in which each site in cortex might represent more than one movement type, the time series of hemodynamic signals was examined in each movement area. Figure 5 shows the time series from 6 representative points on the motor cortex map of subject 1.

Figure 5A shows the time series from a region of cortex dominated by elbow movement. A strong positive hemodynamic response was associated with elbow

movement (green line in time series graph), but a positive hemodynamic response was also present for the forearm and wrist A. Other movement types, including the tongue, lips, and saccadic eye movements, were associated with a reduction in hemodynamic response. The signal at this site in cortex therefore did not solely covary with elbow movement but showed a complex relationship to many movement types. Although it is convenient to label this region of cortex the "elbow representation," the label may be best understood as a short hand for "the cortical area that on average emphasizes the elbow but represents the movement of other body parts as well."

Figure 5B shows the time series from a region of cortex dominated by wrist movement (wrist B, abduction/adduction). A strong positive response was associated with wrist B movement (light blue line in time series graph), and little if any response was associated with other movements.

Figure 5C shows the time series from a region of cortex dominated by finger movement. Although the strongest response was associated with finger movement (red line in time series graph), a positive hemodynamic response was also associated with wrist A, wrist B, and forearm movement. The results therefore do not show a cortical site that represents the fingers exclusively, but instead one that emphasizes the fingers while also representing movement of adjacent joints.

Figure 5D shows the time series from the second wrist representation located ventral to the finger representation. Here again, although the hemodynamic response was strongest during wrist A movement (dark blue line in time series graph), a positive hemodynamic response was also obtained during finger, wrist B, and forearm movement. The data therefore suggest a gradual trend in which a central region emphasizing the

fingers grades into an upper and a lower region emphasizing the more proximal joints of the wrist and forearm.

Figure 5E and F show the time series from cortical sites that emphasize the movement of the upper face during squinting, and the movement of the lips. Once again, it is not the case that each site in cortex is exclusively associated with one movement type. Rather, extensive overlap among movement representations is apparent.

Figure 6 shows time series data from subjects 2-5. Each column shows data from one subject. For example, for subject 2, panels A-E show the time series from 5 sites arranged along the motor map. Panel A shows the time series from a cortical site dorsal to the finger representation, in a cortical region that emphasized wrist movement. In this graph, the largest hemodynamic response is associated with wrist B movement (light blue line). Panel B shows the time series from a cortical site in a transitional area, on the border between the wrist and the finger representation. The hemodynamic responses to wrist movement, forearm movement, and finger movement, are similar. Panel C shows the time series from a cortical site in the finger representation. In this graph, the largest hemodynamic response is associated with finger movement (red line). Panel D shows the time series from another transitional site, this one on the ventral border of the finger representation. Here again the hemodynamic responses to wrist, forearm, and finger movement are similar. Panel E shows the time series from a cortical site ventral to the finger representation, in a cortical area that emphasized forearm movement. Here the hemodynamic response is largest for the forearm movement (pink line). The data from all four subjects displayed in this figure show a similar pattern. A core region emphasized the fingers (Figure 6C, outlined in red). This representation of the fingers graded into two

representations of the wrist and forearm, one just dorsal to the finger representation (Figure 6A) and one just ventral to it (Figure 6E). There was no sharp cutoff between movement representations. Rather, all movement representations were overlapped and within that area of overlap, the emphasis shifted from one type of movement to the next.

Core and surround

The above analyses show that within the large finger and arm representation, there is almost total overlap among the finger and the arm, but that the fingers tend to be relatively emphasized in a central region and the wrist and forearm tend to be relatively emphasized in two areas, one large zone just dorsal to the finger area and one smaller zone just ventral to the finger area. We calculated a "finger-vs-arm" index that showed, for each voxel significantly activated by both the fingers and the arm, whether that voxel was more activated by the fingers, more activated by the arm, or equally activated by both. (See methods for details of index calculation). Figure 7A shows the result for subject 1. This flat map of the central sulcus shows an enlarged view of the cortical region in which a significant hemodynamic response was obtained during movement of the fingers, wrist A, wrist B, and forearm. A red color indicates a hemodynamic signal that covaried predominantly with finger movement (finger-vs-arm index = 1); blue indicates a hemodynamic signal that covaried predominantly with movement of wrist A, wrist B, or forearm (finger-vs-arm index = -1); and intermediate colors indicate a hemodynamic signal that covaried with both categories of movement. The dotted white line shows the floor of the sulcus. The area to the left of the line is the motor cortex. This map shows a core area that emphasized the fingers, a large area just dorsal to the finger

representation that emphasized the more proximal arm joints, and a smaller area just ventral to the finger representation that also emphasized the more proximal arm joints. The finger-arm index shows particularly clearly that these representations are not absolute. There is no central zone dedicated entirely to the fingers, surrounded by zones dedicated entirely to the arm. Instead, in a large area of overlap, the center relatively emphasizes the fingers, and the dorsal and ventral zones relatively emphasize the arm.

The results of subjects 2-5 are shown in Figure 7B-E. These maps are similar in that they show a core region that emphasized the fingers bracketed by a large dorsal and a small ventral region that emphasized more proximal movements. The subjects varied in the extent of this ventral wrist and forearm representation, but all subjects showed at least some cortical area ventral to the core finger area that responded more robustly to the arm than to the fingers.

Group average

To obtain a group average, the maps shown in Figure 7B-E, corresponding to subjects 2-5, were warped according to an affine transformation to align them to the map in Figure 7A. The alignment optimized the correlational match between the finger representations (see methods). Once the maps were aligned, they were averaged. The result is shown in Figure 7F. This group average shows particularly clearly the non-classical organization of the motor cortex in which the fingers are emphasized in a core area, the arm is emphasized in a large area dorsal to the finger representation, and the arm is re-represented in a smaller area just ventral to the finger representation. The group map

also shows the manner in which the representations tend to grade into each other with a change in relative emphasis, rather than forming distinct areas with borders.

Blur across the sulcus

One possible confound in this experiment is blur of signal across the sulcus from the primary somatosensory area to the primary motor area. This blur might occur partly through voxels that straddle the sulcus despite the high resolution of the scan, partly through intrinsic blur in the hemodynamic response, and partly through the smoothing used in our analysis to enhance signal-to-noise. In this manner, the signal from S1 might have contaminated the results from M1.

To address this possible confound, we performed the following analysis. We first defined a mask that included: all voxels that overlapped the posterior bank of the central sulcus, presumed S1; all voxels in the white matter beneath the S1 cortex, within 2 mm of the white-matter/cortex boundary; and all voxels within 2 mm of the pial surface of S1, including voxels that straddled the sulcus and voxels in the superficial layers of the motor cortex. This mask therefore included S1 and a substantial halo of voxels around S1. Before performing any spatial smoothing on the data, we replaced the measured hemodynamic signal in these voxels with randomized noise that contained the same standard deviation but no temporal structure. We then performed the same smoothing and regression analysis described above. In this analysis, M1 was protected from contamination by S1 in the following ways: voxels that straddled the sulcus had had their signal blanked; voxels near S1, that were likely to be contaminated by intrinsic blur in the hemodynamic response, had had their signal blanked; and the spatial smoothing

performed in the analysis could drag only random noise across the sulcus from S1 to M1, perhaps decreasing the signal in M1, but not adding any unwanted signal.

Figure 8 shows the result from subject 1 in the form of a winner-take-all map. This map is directly comparable to the map in Figure 3A, showing data from the same subject. In Figure 8, the posterior bank of the central sulcus shows little signal, as expected, since the signal was removed from S1 at the start of the analysis. The small amount of signal shown in S1 is the result of smoothing across the sulcal wall from M1. M1, in the anterior bank of the central sulcus, shows reduced signal. This reduction is also expected for two reasons. First, the superficial layers of M1, within 2 mm of S1, were blanked of signal. Second, the smoothing algorithm effectively spread statistical noise from the mask into the adjacent M1 voxels, reducing the signal strength. Despite these reduction in signal, the activations in M1 remained robust (the displayed activations crossed a threshold of $P < 0.0001$). The important point of this analysis is that the overall pattern of results remained the same. A somatotopic map is apparent in the primary motor cortex, and the finger area is bracketed dorsally and ventrally by separate wrist and forearm areas. The essential findings, therefore, appear to be independent of signal contamination across the sulcus from S1.

Discussion

High resolution fMRI was used to map the motor cortex in humans. Movements of ten body parts were tested ranging from the toes to the tongue. The results showed a large scale somatotopic map of the body in the motor cortex, as expected, with the tongue

in a ventral location and the toes in a dorsal location. Regions of activation for different body parts overlapped extensively but the somatotopic trend emerged none-the-less. Within the arm and hand representation, however, a non-somatotopic reversal was found. The wrist and forearm were relatively emphasized in two regions, one ventrally and one dorsally to the finger representation. This organization, in which the distal musculature is bracketed by the proximal musculature of the arm, is similar to findings in the monkey motor cortex (Kwan et al. 1978; Park et al. 2001), but different from the classical motor map in the human brain (Penfield and Boldrey 1937). Other functional imaging studies of the human motor cortex obtained an overall somatotopic map but did not report the re-representation of the wrist and forearm (Alkadhi et al. 2002; Lotze et al. 2000; Stippich et al. 2002), perhaps because of the coarse spatial resolution of the imaging techniques used in those studies. In the present study, the high-resolution functional images were of critical importance in resolving the relatively thin strip of wrist and forearm representation ventral to the finger representation.

Representational overlap

A long-standing question in motor cortex research is whether the map of the body in motor cortex is discrete or overlapping. When the first maps of the human motor cortex were published based on electrical stimulation, Foerster (1936) suggested that the primary motor cortex contained discrete, elaborately separated representations of individual body parts, even at the level of individual fingers. In contrast Penfield and Boldrey (1937), using the same method of electrical stimulation, reported that the map was extensively overlapping. In the monkey literature, the debate was resolved in favor

of an overlapping map. Only Asanuma (1975) suggested a map separated at the level of individual muscles. Other researchers (Cheney and Fetz 1980; Donoghue et al. 1992; Gould et al. 1986; Park et al. 2001; Rathelot and Strick 2006; Schieber and Hibbard 1993) obtained highly overlapped maps, and indeed maps that became more overlapped as the animals learned to perform complex movements that integrated among joints (Nudo et al. 1996).

In the more recent imaging literature in humans, the question of overlap has been addressed again. All of the human imaging studies report some degree of overlap among body part representations, but the degree of overlap is still debated. Some researchers suggest that within the overlapped and blurred map, there is a somatotopic trend. For example, individual fingers have hot spots arranged in somatotopic order on the cortex (Beisteiner et al., 2001; Dechent and Frahm, 2003; Kleinschmidt et al., 1997). Others suggest that the motor cortex contains three discrete sectors, one representing the lower body, one representing the midsection, and one representing the head, and that within each sector there is complete overlap and no somatotopic organization (Sanes and Schieber 2001). This second view is in direct contradiction to our data. As shown in Figure 2, within the head representation, although body part representations overlapped, there was nonetheless a clear progression (tongue, lips, squint); and likewise within the arm and hand representation, although body part representations overlapped, there was a clear trend in which different body parts were relatively emphasized in different locations (fingers, wrist, forearm, elbow).

One possible reason for the debate in the human literature is that the extent of overlap among body part representations is difficult to assess using imaging techniques.

There are many possible reasons why cortical activations may overlap. The hemodynamic response itself has an intrinsic spatial imprecision that blurs adjacent movement representations. The movements performed by the subjects may not be entirely separable. For example, when performing a wrist movement, the subject might also wiggle the fingers in a subtle manner. Even if the fingers are stabilized during a wrist movement, this stabilization may be achieved by the active use of finger muscles. For these reasons, although the motor cortex clearly contains extensive representational overlap, the exact amount of overlap may be difficult to assess and should be taken with some caution.

In the present study, adjacent body parts had extensively overlapping representations. This overlap is likely to be largely genuine, since it matches the known properties of the monkey motor cortex. However, it cannot be excluded that some of the representational overlap reported here is the result of blurred signal.

This caveat about representational overlap, however, does not affect the central finding of the present study. We obtained a somatotopic order in which the finger representation is bracketed by two regions that emphasize the arm. The somatotopic order and the reversal in the order cannot be explained by blur in the signal.

Comparison to maps obtained in the human visual system

The technical methods for plotting topographic maps in the human brain have flourished especially in the visual system, where cortical and subcortical retinotopic maps are now routinely plotted. For example, striate and extrastriate visual areas can be distinguished on the basis of their retinotopy (DeYeo et al. 1996; Engel et al. 1997;

Konen and Kastner 2008; Sereno et al. 1995), the lateral geniculate nucleus has been mapped at high resolution (Schneider et al. 2004), the superior colliculus has been mapped (Schneider and Kastner 2005), and cortical eye movement areas including those in the parietal lobe and those in the frontal lobe have been mapped (Kastner et al. 2007; Sereno et al. 2001; Silver et al. 2005). In these experiments, it is understood that each stimulus location in the visual field evokes activity in a distributed region of cortex, and that different stimulus locations result in overlapping regions of cortical activity. The map that is extracted by analysis is a topographic trend, not a punctate map.

In the present study, we borrowed methods now standard in the retinotopic mapping literature including single subject analyses, high resolution scanning, the use of surface reconstructions to evaluate the maps, the use of time series to evaluate the robustness of the activations, and the use of analytical methods to extract a topographic trend from an overlapping set of representations.

Comparison of the core-and-surround organization in monkeys and humans

The present results resemble the core-and-surround organization in the monkey motor cortex but differ in two respects. First, in the monkey, the wrist, forearm, elbow, and shoulder are represented in the cortical belt that surrounds the finger area (Kwan et al. 1978; Park et al. 2001). In the present data, only the wrist and forearm representations bracketed the finger area. Elbow movements did not evoke activity ventral to the hand area. (Shoulder rotations were not tested to avoid head movement.) Second, in the monkey cortex, the hand representation is surrounded ventrally, dorsally, and anteriorly by a continuous strip of cortex that represents the proximal arm muscles. In the present

maps, however, the proximal representation was not clearly a continuous strip but tended to be divided into a large zone dorsal to the hand area and a small zone ventral to the hand area. One possibility is that the two species genuinely differ in these detailed respects. Another possibility is that in the present experiment, the movements tested in the scanner bed were too restrictive to give as complete a map as in the more thorough physiological testing in monkeys. Further mapping of human motor cortex will be needed to clarify the similarities and differences between human and monkey motor maps.

Map organization and "like attracts like"

It has been suggested that a fundamental function of the motor cortex is to integrate the actions of muscles and joints, such that joints that are normally used together are represented together (Donoghue et al. 1992; Nudo et al. 1996; Sanes et al. 1995; Schieber and Hibbard 1993). This integrative hypothesis is one example of a class of hypotheses about the organization of maps. One way to formulate the hypothesis is that "like attracts like." Similar types of information, or processes that are correlated, tend to be mapped near each other in cortex or overlapping each other. Kohonen (1982) incorporated this hypothesis into a formal mathematical model that has been used to explain complex features of topographic maps in the visual system (Durbin and Mitchison 1990). In a recent study we extended the Kohonen method to apply it to the monkey motor cortex (Aflalo and Graziano 2006; Graziano and Aflalo 2007). In that study, we began with an approximate description of a monkey's normal movement repertoire and then used a dimensionality reduction to flatten that highly-dimensional movement repertoire onto a two-dimensional sheet. This process generated a topography

that in many ways resembled the actual topography in a monkey. Body parts that were correlated in the behavioral repertoire became represented in a partially overlapping manner in the model cortex. Furthermore, the somatotopic organization violated a strict body plan. Joints that were not adjacent on the body developed adjacent representations in the model cortex. For example, the representation of the proximal arm joints bracketed the representation of the hand in a manner that violated a strict somatotopy but that matched the pattern observed in the actual motor cortex. This modeling work suggests that at least two features of the monkey motor cortex, the extensive overlapping of representations and the non-somaototopic, core-and-surround organization, might stem partly from the same underlying reason, a maximization of the proximity of representations that frequently interact.

Applying this hypothesis to the human motor cortex is at present difficult. In monkeys, we know a great deal about the statistics of the normal movement repertoire. We also know that different monkeys have extremely similar repertoires. Finally, we know a great deal about the somatotopic details in primary motor, premotor, and supplementary motor cortex. This allows us to make precise comparisons between the complex map expected on the basis of the statistical structure in the repertoire, and the complex map that actually exists in the brain (Aflalo and Graziano 2006; Graziano and Aflalo 2007). In the case of the human, most of this information is lacking. We do not yet have a systematic description of the human movement repertoire. It could be that the repertoire in humans is so varied that, statistically, there is less tight correlation between disparate body parts, leading to less fracturing and duplication in the map. It could be that the repertoire is quite different from person to person, leading to complex fractures in the

map that are, however, not consistent among subjects. The present results suggest that at least one reversal in the map is present and consistent across people. Thus, in principle, some factors other than somatotopy are probably in play. However, at this point, it is difficult to determine whether complexities in the human movement repertoire are responsible for this reversal in the map. Answering these questions will require a better understanding of the statistical structure of the human motor repertoire, and also a mapping of the human motor cortex in terms of behaviorally meaningful actions rather than in terms of simple joint rotations.

Acknowledgements

We thank Megan Harvey and Sara Szczepanski for help in running subjects and analyzing data. We thank Theodore Mole for comments on the manuscript. Supported by NIH grants R01 NS-046407, R01 MH-64043, and P50 MH-62196.

References

Aflalo TN, Graziano MSA. Possible origins of the complex topographic organization of motor cortex: reduction of a multidimensional space onto a 2-dimensional array. J Neurosci 26: 6288-6297, 2006.

Alkadhi H, Crelier GR, Boendermaker SH, Golay X, Hepp-Reymond MC, Kollias SS. Reproducibility of primary motor cortex somatotopy under controlled conditions. AJNR Am J Neuroradiol 23: 1524-1532, 2002.

Asanuma H. Recent developments in the study of the columnar arrangement of neurons within the motor cortex. Physiol Rev 55: 143-156, 1975.

Beisteiner R, Windischberger C, Lanzenberger R, Edward V, Cunnington R, Erdler M, Gartus A, Streibl B, Moser E, Deecke L. Finger somatotopy in human motor cortex. Neuroimage 13: 1016-1026, 2001.

Cheney PD, Fetz EE. Comparable patterns of muscle facilitation evoked by individual corticomotoneuronal (CM) cells and by single intracortical microstimuli in primates: evidence for functional groups of CM cells. J Neurophysiol 53: 786-804, 1985.

Cox RW. AFNI: Software for analysis and visualization of functional magnetic resonance neuroimages. Comput Biomed Res 29: 162-173, 1996.

Cox RW, Jesmanowicz A. Real-time 3D image registration for functional MRI. Magn Reson Med 42: 1014-1018, 1999.

Cusack R, Brett M, Osswald K. An evaluation of the use of magnetic field maps to undistort echo-planar images. Neuroimage 18: 127-142, 2003.

Dale AM, Fischl M, Sereno MI. Cortical surface-based analysis. I. Segmentation and surface reconstruction. Neuroimage 9: 179-194, 1999.

Dechent P, Frahm J. Functional somatotopy of finger representations in human primary motor cortex. Hum Brain Mapp 18: 272-283, 2003.

DeYoe EA, Carman GJ, Bandettini P, Glickman S, Wieser J, Cox R, Miller D, Neitz J. Mapping striate and extrastriate visual areas in human cerebral cortex. Proc Natl Acad Sci USA 93: 2382-2386, 1996.

Donoghue JP, Leibovic S, Sanes JN. Organization of the forelimb area in squirrel monkey motor cortex: representation of digit, wrist, and elbow muscles. Exp Brain Res 89: 1-19, 1992.

Durbin R, Mitchison G. A dimension reduction framework for understanding cortical maps. Nature 343: 644-647, 1990.

Engel SA, Glover GH, Wandell BA. Retinotopic organization in human visual cortex and the spatial precision of functional MRI. Cereb Cortex 7: 181-192, 1997.

Fischl M, Sereno MI, Dale AM. Cortical surface-based analysis. II: Inflation, flattening, and a surface-based coordinate system. Neuroimage 9: 195-207, 1999.

Foerster O. The motor cortex of man in the light of Hughlings Jackson's doctrines. Brain 59: 135-159, 1936.

Gonzalez RC, Woods RE. Digital Image Processing. Prentice Hall, Upper Saddle River, NJ: 2002.

Gould HJ, Cusick CG, Pons TP, Kaas JH. The relationship of corpus callosum connections to electrical stimulation maps of motor, supplementary motor, and the frontal eye fields in owl monkeys. J Comp Neurol 247: 297-325, 1986.

Graziano MSA, Aflalo TN. Mapping behavioral repertoire onto the cortex. Neuron 56: 239-251, 2007.

Graziano MSA, Taylor CSR, Moore T. Complex movements evoked by microstimulation of precentral cortex. Neuron 34: 841-851, 2002.

Hlustik P, Solodkin A, Gullapalli RP, Noll DC, Small SL. Somatotopy in human primary motor and somatosensory hand representations revisited. Cereb Cortex 11: 312-321, 2001.

Indovina I, Sanes JN. On somatotopic representation centers for finger movements in human primary motor cortex and supplementary motor area. Neuroimage 13: 1027-1034, 2001.

Kleinschmidt A, Nitschke MF, Frahm J. Somatotopy in the human motor cortex hand area. A high-resolution functional MRI study. Eur J Neurosci 9: 2178-2186, 1997.

Kastner S, DeSimone K, Konen CS, Szczepanski SM, Weiner KS, Schneider KA. Topographic maps in human frontal cortex revealed in memory-guided saccade and spatial working-memory tasks. J Neurophysiol 97: 3494-3507, 2007.

Kohonen T. Self-organizing formation of topologically correct feature maps. Biol Cybernetics 43: 59-69, 1982.

Konen CS, Kastner S. Two hierarchically organized neural systems for object information in human visual cortex. Nat Neurosci 11: 224-231, 2008.

Kwan HC, MacKay WA, Murphy JT, Wong YC. Spatial organization of precentral cortex in awake primates. II. Motor outputs. J Neurophysiol 41: 1120-1131, 1978.

Lotze M, Erb M, Flor H, Huelsmann E, Godde B, Grodd W. fMRI evaluation of somatotopic representation in human primary motor cortex. Neuroimage 11: 473-481, 2000.

Nudo RJ, Milliken GW, Jenkins WM, Merzenich MM. Use-dependent alterations of movement representations in primary motor cortex of adult squirrel monkeys. J Neurosci 16: 785-807, 1996.

Park MC, Belhaj-Saif A, Gordon M, Cheney PD. Consistent features in the forelimb representation of primary motor cortex in rhesus macaques. J Neurosci 21: 2784-2792, 2001.

Penfield W, Boldrey E. Somatic motor and sensory representation in the cerebral cortex of man as studied by electrical stimulation. Brain 60: 389-443, 1937.

Rathelot JA, Strick PL. Muscle representation in the macaque motor cortex: an anatomical perspective. Proc Natl Acad Sci USA 103: 8257-8262, 2006.

Sanes JN, Donoghue JP, Thangaraj V, Edelman RR, Warach S. Shared neural substrates controlling hand movements in human motor cortex. Science 268: 1775-1777, 1995.

Sanes JN, Schieber MH. Orderly somatotopy in primary motor cortex: does it exist? Neuroimage 13: 968-974, 2001.

Schieber MH, Hibbard LS. How somatotopic is the motor cortex hand area? Science 261: 489-492, 1993.

Schneider KA, Kastner S. Visual responses of the human superior colliculus: a high-resolution functional magnetic resonance imaging study. J Neurophysiol 94: 2491-2503, 2005.

Schneider KA, Richter MC, Kastner S. Retinotopic organization and functional subdivisions of the human lateral geniculate nucleus: a high-resolution functional magnetic resonance imaging study. J Neurosci 24: 8975-8985, 2004.

Sereno MI, Dale AM, Reppas JB, Kwong KK, Belliveau JW, Brady TJ, Rosen BR, Tootell RB. Borders of multiple visual areas in humans revealed by functional magnetic resonance imaging. Science 268: 889-893, 1995.

Sereno MI, Pitzalis S, Martinez A. Mapping of contralateral space in retinotopic coordinates by a parietal cortical area in humans. Science 294: 1350-1354, 2001.

Sessle BJ, Wiesendanger M. Strucutal and functional definition of the motor cortex in the monkey (Macaca fascicularis). J Physiol 323: 245-265, 1982.

Stippich C, Ochmann H, Sartor K. Somatotopic mapping of the human primary sensorimotor cortex during motor imagery and motor execution by functional magnetic resonance imaging. Neurosci Lett 331: 50-54, 2002.

Silver MA, Ress D, Heeger DJ. Topographic maps of visual spatial attention in human parietal cortex. J Neurophysiol 94: 1358-1371, 2005.

Woolsey CN, Settlage PH, Meyer DR, Sencer W, Hamuy TP, Travis AM. Pattern of localization in precentral and "supplementary" motor areas and their relation to the concept of a premotor area. In: Association for Research in Nervous and Mental Disease 30, 238-264. New York: Raven Press, 1952.

Figure legends

Figure 1: Hemodynamic response function based on data from subject 1. Signals from 40 voxels throughout motor cortex were used. Each individual time series was normalized to a peak value of 1. The individual, normalized time series were then averaged to obtain the mean hemodynamic response function. Error bars are standard deviation.

Figure 2: Cortical activations evoked by ten different movement types in subject 1. Displayed on an inflated cortical sheet are β values obtained by regression against the ten movement types, thresholded at $P < 0.0001$ uncorrected, only positive β values displayed. Warm colors indicate greater beta values and cold colors indicate smaller beta values. The β values are expressed in units of percent signal change. Thus a β value of 1 indicates that, according to the regression analysis, the movement caused a peak-to-peak change in signal intensity of 1%. The scale was truncated at 2%. All displays are of a lateral view of the left hemisphere except for panel I which shows a dorsal view.

Figure 3: Somatotopy in subject 1 displayed in a “winner-take-all” map. A, Data from first scan session. B, Data from second scan session, 2 months later. Voxels were selected

if the regression was positive and significant at the $P < 0.0001$ level. These selected voxels where then assigned to the movement that resulted in the largest F value. The results were then projected onto the inflated cortical sheet, in which dark shading indicates the floor of a sulcus and light shading indicates the crown of a sulcus. The map shows the overall somatotopic progression in the primary motor cortex (anterior to the floor of the central sulcus) and in the primary somatosensory cortex (posterior to the floor of the central sulcus).

Figure 4: Somatotopy displayed in a "winner-take-all" map. A-D, Data from subjects 2-5.

Figure 5: Time series data for subject 1. The cortical map shows a close-up of the winner-take-all display of the motor cortex (see Figure 3A). A-F, hemodynamic time series for the ten movement conditions, for each of the indicated points on the cortex. Time series were based on unsmoothed data, and were a mean of 5 adjacent voxels within the cortical slab. The percent signal change was normalized to the initial value in the plotted time interval. Error bars are standard deviations. The blue rectangle indicates the time during which the movement was performed.

Figure 6: Time series data for subjects 2-5. Each column shows data from a different subject. Each row shows data from a different location along the motor cortex map. A, Data from a dorsal location in the upper wrist/forearm representation. B, Data from a transitional location between the upper wrist/forearm representation and the finger representation. C, Data from the center of the finger representation. D, Data from a

transitional location between the lower wrist/forearm representation and the finger representation. E, Data from a ventral location in the lower wrist/forearm representation. The color scheme for indicating specific movement types is the same as in Figure 5.

Figure 7: Core-and-surround organization of the hand and arm representation in five individual subjects and in a group average of subjects. Each panel shows a close-up of the flattened motor cortex. The width of each panel represents approximately 4 cm. A. Those voxels that showed hemodynamic responses to the fingers, wrist, or forearm, and that were significant at $P < 0.0001$, were selected for further analysis. For each selected voxel, a finger-vs-arm index was calculated in which –1 indicated a response to the wrist and forearm but not to the fingers, +1 indicated a response to the fingers but not to the wrist and forearm, and 0 indicated an equal response to both. The results were projected onto an inflated cortical surface, with red indicating +1 and dark blue indicating –1. The white dotted line shows the floor of the central sulcus, with the primary motor cortex to the left of the line. B-E, Same for remaining subjects. F, Mean result obtained by first aligning the finger representations of the five subjects and then averaging the finger-vs-arm indices.

Figure 8: Result for subject 1 when signal in primary somatosensory cortex was removed prior to analysis. For all voxels in S1 or within 2 mm of S1, the measured hemodynamic signal was replaced with noise that had the same standard deviation and mean but no temporal structure. After smoothing and regression analysis, a similar result was obtained in M1, though the amount of signal in M1 was reduced (compare to Figure 3A). The

result suggests that the findings in M1 were not the result of signal contamination across the sulcus from S1.

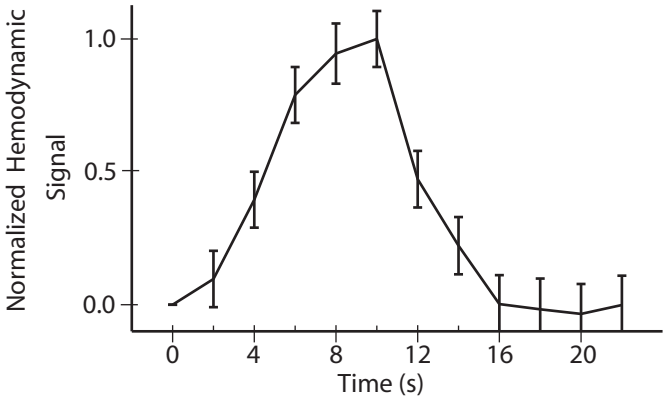

Figure 1
1 column
Meier et al.

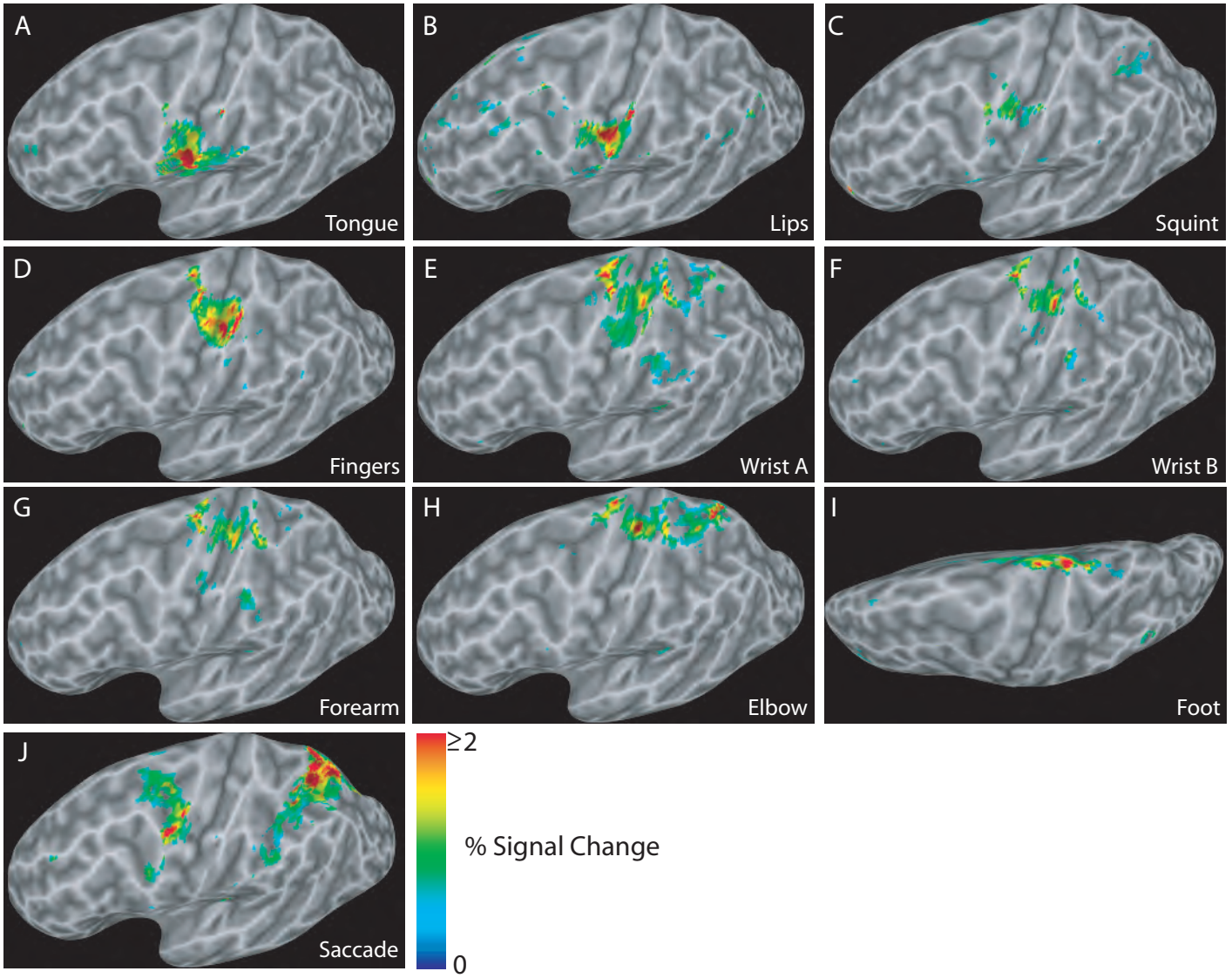

Figure 2
2 columns
Meier et al.

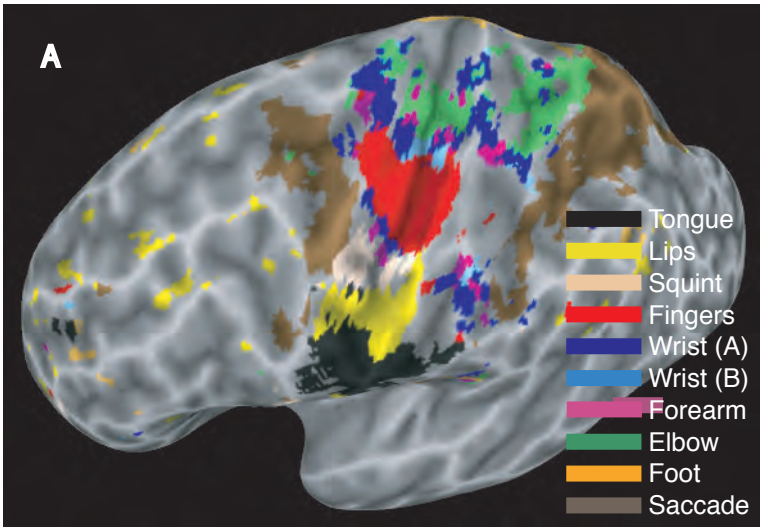

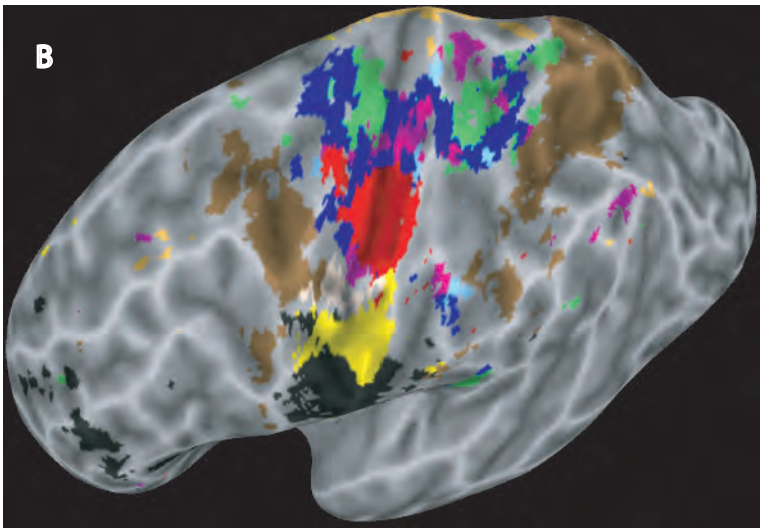

Figure 3
1 column
Meier et al.

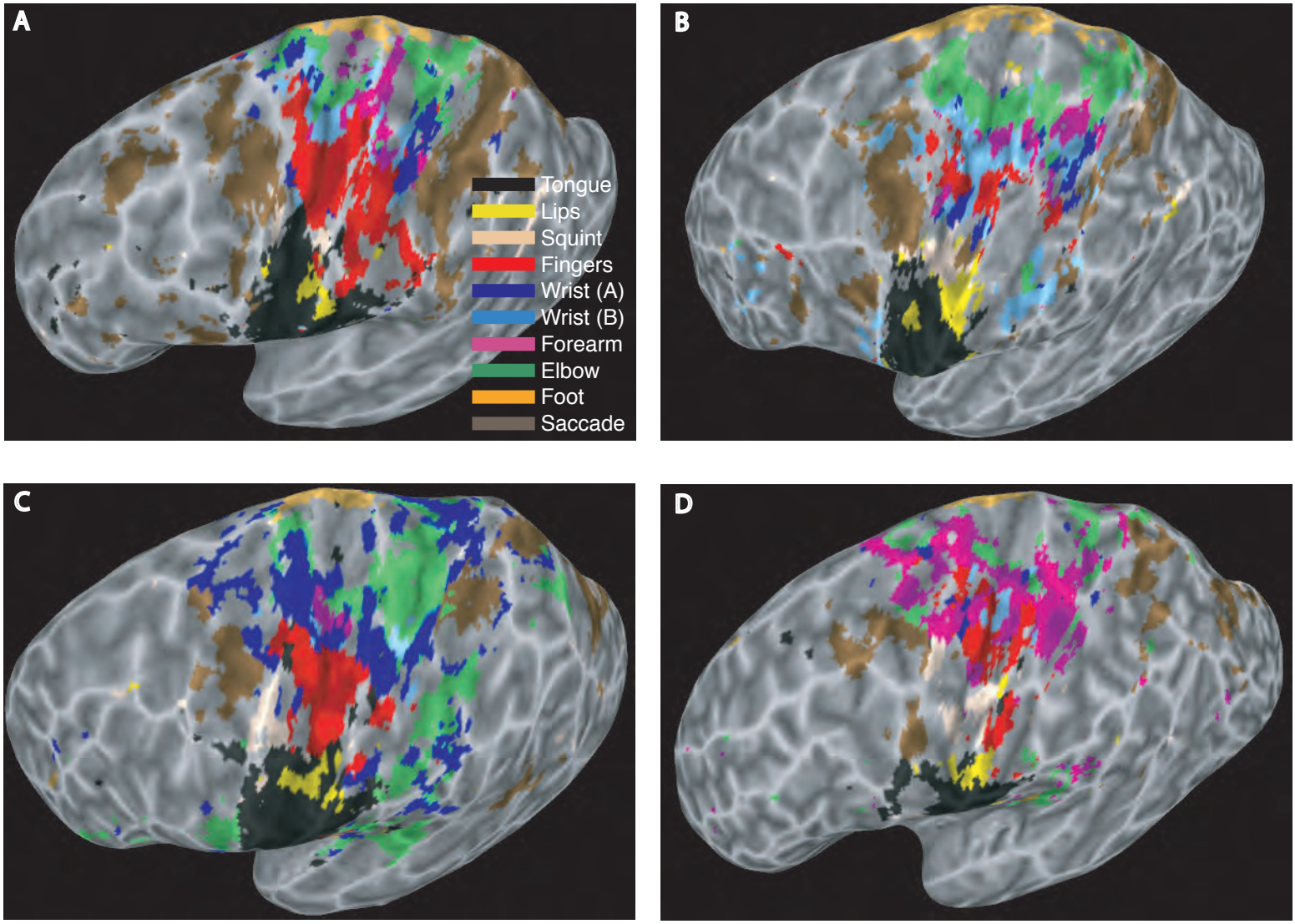

FIgure 4
2 columns
Meier et al.

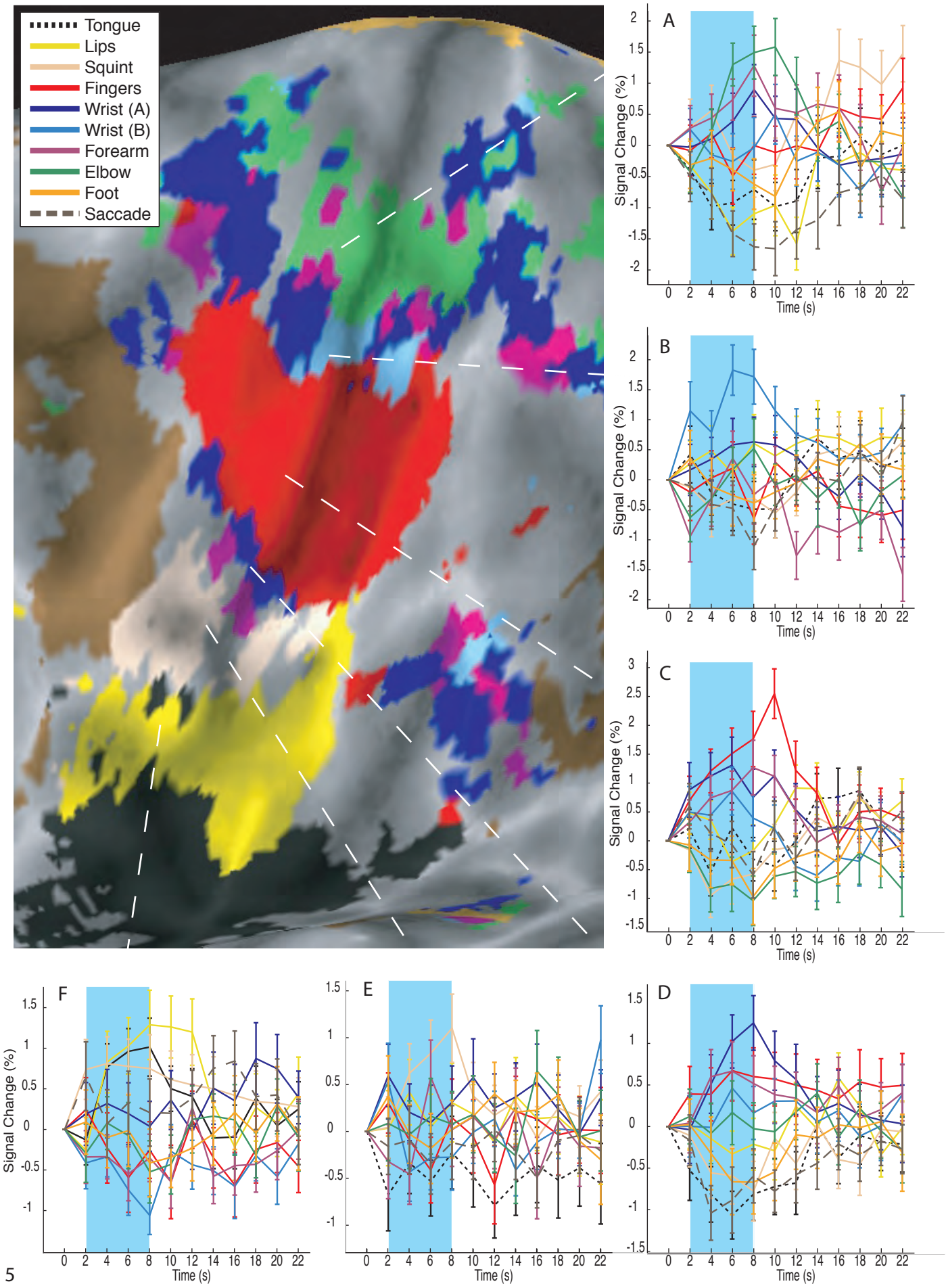

Figure 5
2 columns
Meier et al.

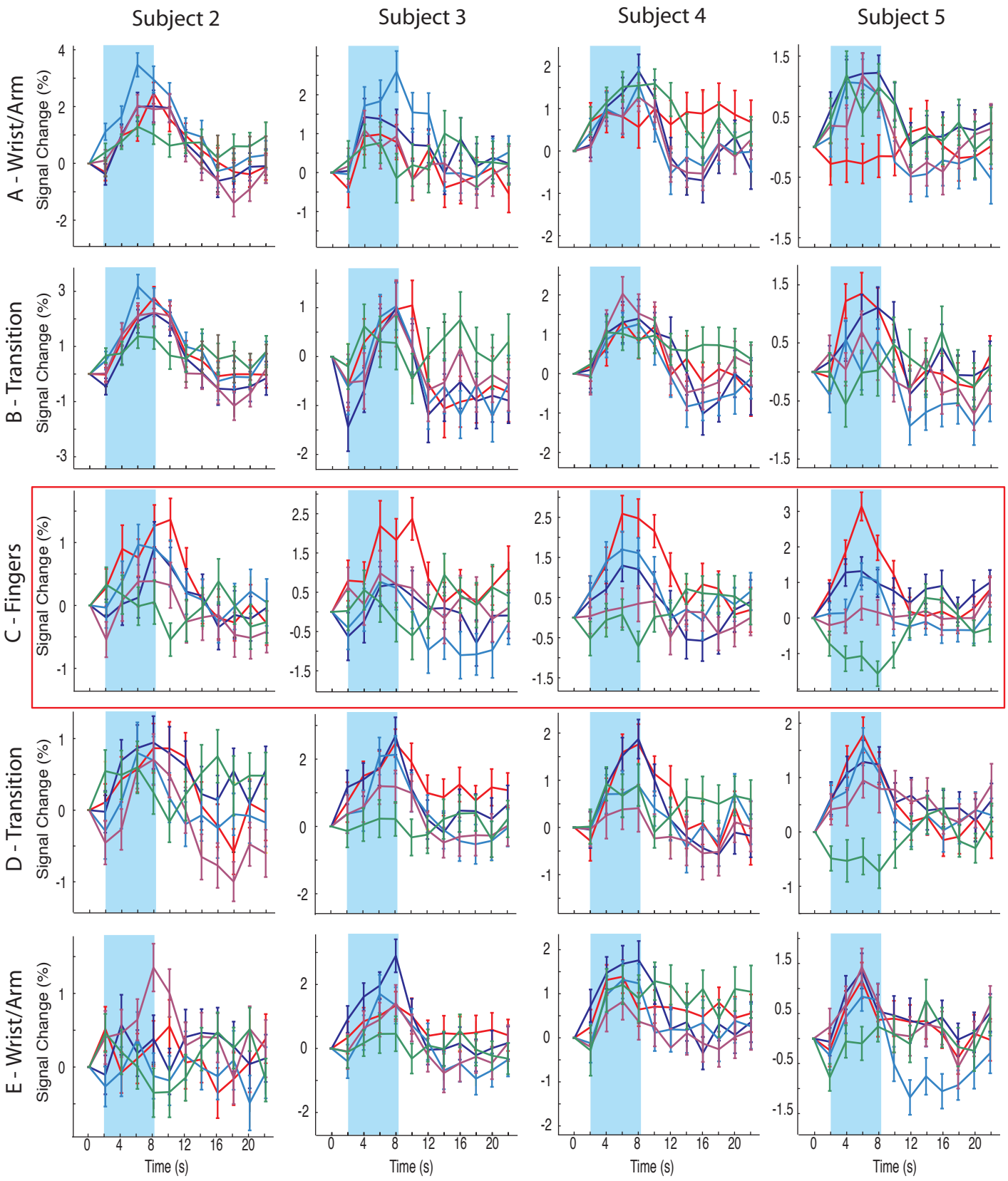

Figure 6
2 columns
Meier et al.

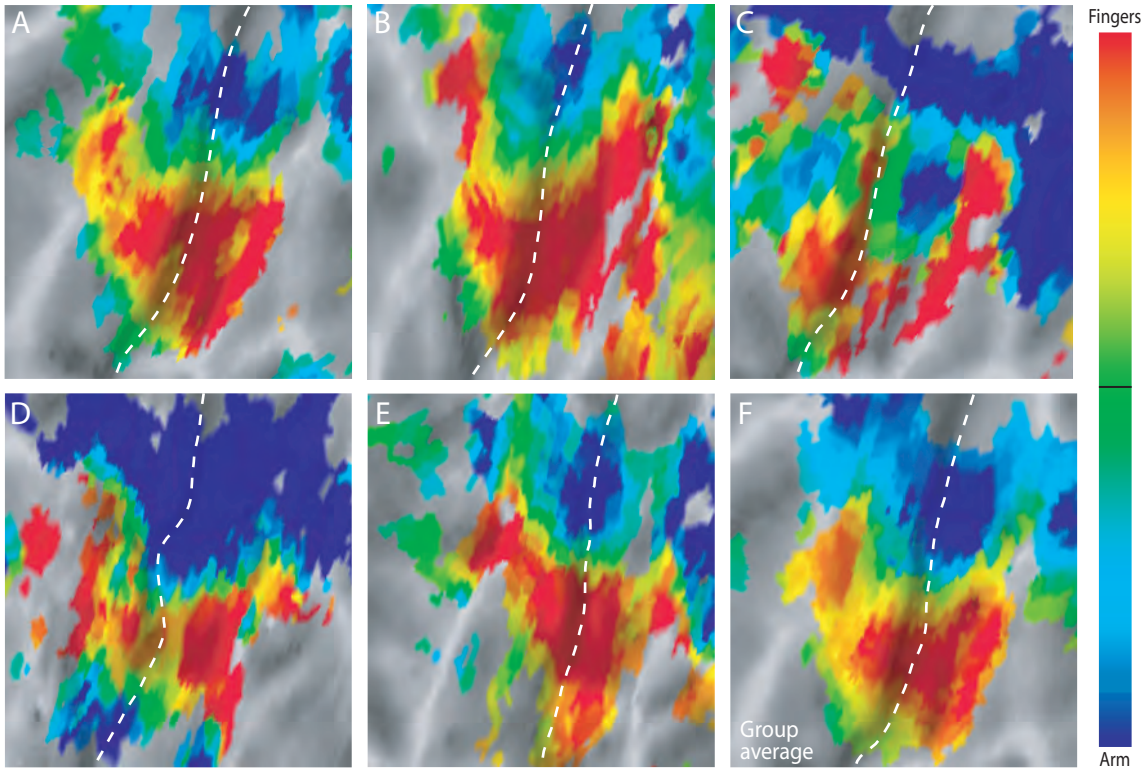

Figure 7
2 columns
Meier et al.

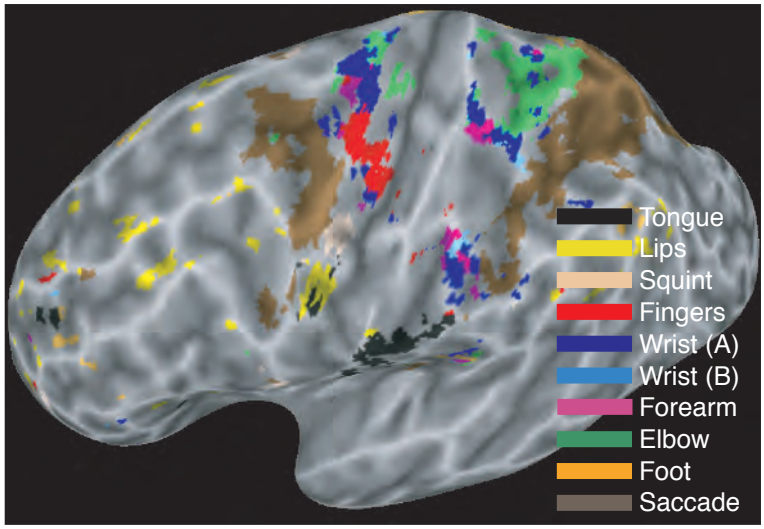

Figure 8
1 column
Meier et al.